Inorganica Chimica Acta, *156* (1989) 257–264

Structure, Electrical and Spectroscopic Properties of Tetrathiafulvalene (TTF)–Thiocyanate Complexes, $(TTF)Cu(SCN)_2$ and $(TTF)(SCN)_{0.66}$

GLORIA J. PYRKA, QUINTUS FERNANDO*
Department of Chemistry, University of Arizona, Tucson, AZ 85721, U.S.A.
MICHIKO B. INOUE and MOTOMICHI INOUE*
CIPM, Universidad de Sonora, AP 130, Hermosillo, Sonora, Mexico

(Received April 11, 1988; revised July 18, 1988)

Abstract

Electrochemical oxidation of TTF by the use of a solution of tetrahydrofuran containing CuSCN and NH_4SCN yielded $(TTF)Cu(SCN)_2$ and $(TTF)(SCN)_{0.66}$. The former was a poor electrical conductor with conductivity *ca.* 10^{-8} S cm^{-1}, whereas the electrical conductivity of the latter was 100–700 S cm^{-1} at 300 K and exhibited a metallic temperature dependence above *ca.* 200 K. $(TTF)Cu(SCN)_2$ crystallized in the monoclinic space group $P2_1/c$ with cell parameters, $a = 8.846(1)$, $b = 9.974(1)$, $c = 15.412(2)$ Å and $\beta = 106.15(1)°$. Ambidentate thiocyanate linkages formed a two-dimensional puckered sheet. A close face-to-face stack of TTF was formed only between pairs of TTFs. $(TTF)(SCN)_{0.66}$ crystallized in the tetragonal space group $P\bar{4}n2$ with the cell dimensions $a = 11.225(1)$ and $c = 3.631(1)$ Å, and was isostructural with the known compounds $(TTF)(SCN)_{0.58}$ and $(TTF)Cl_{0.8}Cu_{0.66}$. The inorganic ions are disordered; detailed structure determination was difficult. $TTF^{+\cdot}$ moieties stacked face-to-face with the interplanar distance 3.631 Å. Charge transport properties, infrared and electron spin resonance spectra of $(TTF)Cu(SCN)_2$ and $(TTF)(SCN)_{0.66}$ reflected the difference observed in the structure.

Introduction

A direct redox reaction of copper(II) halides with tetrathiafulvalene (TTF) or its analogs yields a variety of charge transfer complexes that incorporate copper halide anions as acceptors: $(TTF)_nCuX_2$ (X = Cl, Br or I) [1, 2], $(TTF)CuCl_4$ [3], $(TTF)CuBr_3$ [3], $(DBTTF)CuX_3$ (DBTTF = dibenzotetrathiafulvalene; X = Cl or Br) [4, 5], $(BEDTTTF)_nCuX_2$ (BEDTTTF = bis(ethylenedithio)tetrathiafulvalene; X = Cl or Br) [6], $(BEDTTTF)CuCl_2$ [7], and $(TMTSF)_nCuX_2$ (TMTSF = tetramethyltetraselenafulvalene; X = Cl or Br) [8]. On the other hand, $(BEDTTTF)_2CuCl_2$ has been electrochemically prepared using $[(n\text{-}C_4H_9)_4N]CuCl_2$ solutions as electrolyte [9]. The mode of the donor stack and the charge occupation of the donor molecules are different from one compound to another so that the electrical and magnetic properties of the compounds are quite different [1–11]. The charge occupation of the donor is related to the redox potential difference between donor and acceptor, and the mode of donor stack is governed by the geometry of the acceptor counterion. The redox potential of copper varies over a wide range depending on the nature of coordinated halide ions, and, moreover, the coordination geometries of corresponding copper(I) and copper(II) compounds are quite different [1, 12]. The use of copper complex anions as acceptors, therefore, yields varying charge transfer complexes with the sulfur-based donors. These findings have prompted us to study new TTF–copper complexes with the different kinds of coordinated ligands. In the present investigation, we have carried out the electrochemical oxidation of TTF using a mixture of CuSCN and NH_4SCN in THF as the electrolyte, and we have obtained $(TTF)Cu(SCN)_2$ and $(TTF)(SCN)_{0.66}$. We report below the structures, and the electrical and spectroscopic properties of the two compounds.

Experimental

Electrocrystallization

The crystals were prepared electrochemically by the use of an H-shaped two-compartment cell with Pt electrodes. TTF (20 mg) was placed in the anode compartment and a deaerated THF (20 ml) solution containing CuSCN (120 mg) and NH_4SCN (150 mg) was loaded in both compartments. The mole ratio of NH_4SCN:CuSCN used was 2:1; the copper compound was not sufficiently soluble when an equimolar ratio of the ammonium salt was used. The

---

*Authors to whom correspondence should be addressed.

0020-1693/89/$3.50

crystallization was performed under a galvanostatic condition in the absence of light. Dark blue multifaceted prisms were formed in the horizontal part of the H cell, and black needles were grown on the electrode. The former was characterized as (TTF)-$Cu(SCN)_2$ and the latter was found to be (TTF)-$(SCN)_{0.66}$ as described later.

X-ray Crystallography

Blue prisms, (TTF)Cu(SCN)$_2$

A dark blue multifaceted prism approximately 0.37 mm X 0.33 mm X 0.22 mm was mounted on a glass fiber. The density was measured by flotation in aqueous zinc bromide; $D_m = 1.96$ g cm^{-3} and $D_c = 1.95$ g cm^{-3}. The data collection was performed with a Nicolet/Syntex $P2_1$ diffractometer using Mo Kα radiation ($\lambda = 0.71073$ Å) and a graphite crystal, incident beam monochromator. The cell constants were determined from 25 reflections in the range $25° < 2\theta < 35°$. The unit cell was monoclinic with cell parameters $a = 8.846(1)$, $b = 9.974(1)$, $c = 15.412(2)$ Å, $\beta = 106.15(1)°$, $V = 1306.1$ Å^3. The space group was found to be $P2_1/c$. The $2\theta/\theta$ scan method with a variable scan rate from 2° to 8°/min was used to collect the data. Three standard reflections that were collected after every 46 reflections had a standard deviation of 1.5%. The linear absorption coefficient was 25.7 cm^{-1}. Both an analytical and an empirical absorption correction were attempted, but no improvement was obtained from either. The data were corrected for Lorentz and polarization effects.

2628 reflections with $2\theta < 50°$ were measured of which 2150 were unique. Intensities of equivalent reflections were averaged. Six reflections were rejected from the averaging process because their intensities differed significantly from the average. The agreement factor for the averaging of the 280 observed and accepted reflections was 1.7% based on intensity and 1.2% based on Fo. The direct method MULTAN program was used to locate the copper and the six unique sulfur atoms. The remaining carbon and nitrogen atoms were located with Fourier techniques. The positions of the hydrogen atoms were calculated geometrically. The hydrogen coordinates were not refined. 1981 reflections with intensities greater than $3\sigma(I)$ were used in a full-matrix least-squares refinement of 154 parameters where $\Sigma w(|F_o| - |F_c|)$ was minimized; w was calculated from $w = 4F/\sigma^2(F^2)$. The refinement converged with $R = 0.032$ and $R_w = 0.040$. The ratio of maximum least-squares shift to error was 0.02. The largest peak in the difference map was 0.42(11) e/Å^3. The scattering factors used were from Cromer and Waber [13] and anomalous dispersion effects were included in the values of F_c; the values of Wf' and Wf'' were from Cromer [14]. All calculations were performed on a PDP-11 computer with the software package SDP-PLUS (Enraf-Nonius & B. A. Frenz & Associates, Inc.).

Black needles, (TTF)(SCN)$_{0.66}$

A black rectangular prism approximately 0.15 mm X 0.08 mm X 0.50 mm was mounted on a glass fiber. The density was measured by flotation in aqueous zinc bromide; $D_m = 1.71$ g cm^{-3}. The cell constants were determined from 25 reflections in the range $21° < 2\theta < 35°$. The unit cell was tetragonal with cell parameters $a = 11.225(1)$, $c = 3.631(1)$ Å, $V = 475.5(1)$ Å^3. The space group was found to be $P\bar{4}n2$. Three standard reflections that were collected after every 46 reflections had a standard deviation of 2.7%. The linear absorption coefficient was 14.0 cm^{-1}. No absorption correction was attempted. The data were corrected for Lorentz and polarization effects.

1235 reflections with $2\theta < 65°$ were measured of which 1020 were unique. Intensities of equivalent reflections were averaged. The agreement factor for the averaging of the 147 observed and accepted reflections was 0.8% based on intensity and 1.2% based on F_o. The tetrathiafulvalene sulfur was located from the Patterson function. The remaining TTF carbon and hydrogen atoms were located with Fourier techniques. The electron density corresponding to the thiocyanate anions had uniform cylindrical symmetry about the c axis. The column of electron density was fitted with a single sulfur atom at $x = y = z = 0$ with highly anisotropic thermal parameters and a multiplicity of 0.26, which is not significantly different from the value of 0.25 which is demanded by the symmetry of the space group. Several other arrangements of sulfur, carbon and nitrogen were attempted. None of these refinements converged, as would be expected from the uniformity of the electron density along the c axis. The hydrogen coordinates were not refined. 431 reflections with intensities greater than $3\sigma(I)$ were used in a full-matrix least-squares refinement of 28 parameters where $\Sigma w(|F_o| - |F_c|)$ was minimized; w was calculated from $w = 4F/\sigma^2(F^2)$. The refinement converged with $R = 0.038$ and $R_w = 0.049$. The ratio of maximum least-squares shift to error was 0.25. The largest peak in the difference map was 0.33(7) e/Å^3.

The analytical data of the crystals indicated that the compound formula was (TTF)$(SCN)_{0.66}$. Calc.: C, 32.96; H, 1.66; N, 3.81. Found: C, 32.25; H, 1.69; N, 3.79%. The space group is the same as that of the known compound $(TTF)_{11}(SCN)_6$ [or (TTF)-$(SCN)_{0.55}$] that has the space group $P\bar{4}n2$ and the corresponding cell constants are almost identical with each other: $a = b = 11.205$ and $c = 3.632$ Å in (TTF)$(SCN)_{0.55}$ [15]. The black needles were, therefore, assumed to be isostructural with (TTF)-$(SCN)_{0.55}$.

Physical Measurements

The crystal conductivity of the black needles was determined by the standard four-probe method along the needle axis. Pt wires of 0.025 mm diameter were connected to a sample crystal with Aquadag.

The conductivity of the prisms was measured by the two-probe method; the room temperature conductivity was of the order of 10^{-8} S cm^{-1} along all crystal orientations investigated.

The infrared (IR) spectra were recorded with Nujol and Fluorolube mulls of the compound and by the use of a Perkin-Elmer 1420 spectrometer.

The electron spin resonance (ESR) spectra were obtained with the aid of a Varian E3 spectrometer. Diphenylpicrylhydrazyl (DPPH) or Mn^{2+}/MgO was used for calibration in the determination of g values.

A Vacuum Generator ESCALAB MKII spectrometer (E. Grinstead, U.K.) was used to obtain the XPS spectra. Crystals were ground into a powder and pressed onto indium foil. The binding energies of the photoelectrons were calculated from the Auger parameter measured for copper, and the copper $2p_{1/2}$ peak was assumed to be 932.4 eV. The digitally recorded data were signal averaged until an acceptable signal:noise level was obtained. The pressure in the sample chamber remained below 5×10^{-10} torr during the experiment. No significant outgassing of the sample occurred. There was no indication of sample decomposition due to X-ray irradiation.

Results

Blue Prisms, (TTF)Cu(SCN)$_2$

The single crystal X-ray structure determination indicated that the dark blue prism was (TTF)Cu(SCN)$_2$, which consists of tetrathiafulvalenium cations within a two dimensional infinite network of copper(I) thiocyanate anions. The lattice is formally composed of four $[Cu(SCN)_2]^-$ anions per unit cell. Each copper has four ambidentate thiocyanate ions coordinated to it in a distorted tetrahedral configuration. Two of these thiocyanates are bonded through the sulfur and two are bonded through the nitrogen. Two adjacent copper atoms are bridged by two SCN^- ions, and form a puckered eight-membered ring. The remaining thiocyanates link the copper–thiocyanate rings into a two dimensional infinite sheet. This can best be seen in the ORTEP stereo view of the unit cell shown in Fig. 1. A similar structure has been reported for tris(2-pyrazolylethyl)-amine copper thiocyanate (Cu(NCS)(tpea)) [16]. Table 1 contains the final positional and isotropic thermal parameters. Tables 2 and 3 contain the bond lengths and bond angles, respectively.

The two Cu–S bond lengths are nearly equal with the longer of the two being part of the eight-membered ring. The ring Cu–SB–CB angle is 97.1°, which is significantly smaller than the 102.4° for the Cu–SA–CA angle. The angles between the thiocyanate groups range from 105.6° to 112.8°. The Cu(NCS)(tpea) structure exhibits a more distorted tetrahedral coordination sphere around the copper, where the thiocyanate angles are between 102.6° and 126.5°. The largest difference between the two infinite networks occurs for the NA–Cu–NB angle. With the tetrathifulvalenium salt the angle is 108.3°, whereas, in Cu(NCS)(tpea) the angle is 126.5°. The copper–thiocyanate lattice spans a rectangle of dimensions $b \times c$, and is sufficiently flexible to be able to accommodate cations of different sizes. The angles of the thiocyanates around the copper distort to fit slightly different crystallographic lattice parameters (8.847 × 16.302 Å for Cu(NCS)(tpea) and 9.974 × 15.412 Å for (TTF)Cu(SCN)$_2$). This corresponds to an area of 144 Å^2 and 154 Å^2, respectively.

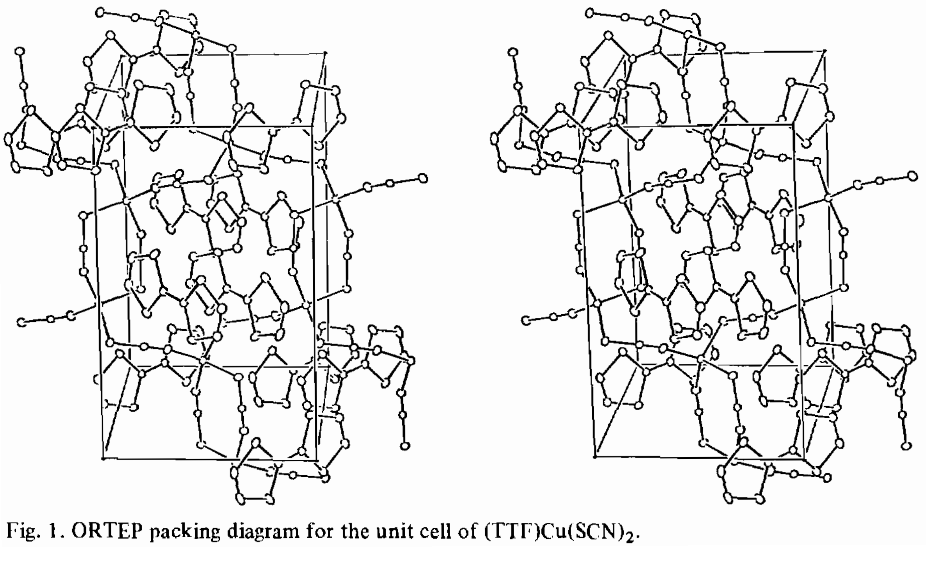

Fig. 1. ORTEP packing diagram for the unit cell of (TTF)Cu(SCN)$_2$.

TABLE 1. Positional Parameters[a] and Isotropic Thermal Parameters[b] of $(TTF)Cu(SCN)_2$

Atom	x	y	z	B (Å^2)
Cu	0.50713(5)	0.07439(4)	0.33954(2)	2.801(8)
SA	0.7040(1)	−0.00547(8)	0.27458(6)	3.15(2)
SB	0.33626(9)	−0.11100(8)	0.34362(5)	2.64(1)
CA	0.6466(3)	−0.1616(3)	0.2471(2)	2.41(6)
CB	0.3726(3)	−0.1195(3)	0.4538(2)	2.00(5)
NA	0.3930(3)	0.2316(3)	0.2738(2)	3.30(6)
NB	0.6018(3)	0.1269(3)	0.4681(2)	2.83(5)
S1	0.02289(9)	0.27999(8)	0.05824(5)	2.92(2)
S1′	−0.27396(9)	−0.01205(8)	−0.11907(5)	2.70(2)
S2	−0.0395(1)	0.22449(9)	−0.13313(5)	3.21(2)
S2′	−0.21843(9)	0.04054(8)	0.07337(5)	2.63(1)
C1	0.1244(4)	0.3722(3)	−0.0010(3)	3.51(7)
C1′	−0.3707(3)	−0.1125(3)	−0.0612(2)	2.80(6)
C2	0.0947(4)	0.3480(3)	−0.0889(3)	3.72(8)
C2′	−0.3439(4)	−0.0889(3)	0.0264(2)	2.81(6)
C3	−0.0772(3)	0.1848(3)	−0.0329(2)	2.23(6)
C3′	−0.1783(3)	0.0814(3)	−0.0261(2)	2.13(6)
H1	0.194	0.443	0.032	5.0
H1′	−0.444	−0.170	−0.092	5.0
H2	0.149	0.397	−0.128	5.0
H2′	−0.386	−0.146	0.061	5.0

[a]Hydrogen atoms were not refined. [b]Anisotropically refined atoms are given in the form of the isotropic equivalent thermal parameter defined as: $8\pi^2(U_{11} + U_{22} + U_{33})/3$.

The SCN–Cu–SCN angles around the copper for the TTF complex are closer to the expected tetrahedral angle, which indicates the lattice distorts less to accommodate the smaller cation.

The tetrathiafulvalenium cation does not lie on a symmetry element in the $P2_1/c$ space group. The bond distances and angles indicate that the molecule possesses nearly D_{2h} symmetry. The cation is planar with the largest deviation from the plane being 0.04 Å.

TABLE 2. Bond Lengths (Å) for $(TTF)Cu(SCN)_2$

Atom	Atom	Distance (Å)	Atom	Atom	Distance (Å)
Cu	SA	2.375(1)	SA	CA	1.656(3)
Cu	SB	2.400(1)	SB	CB	1.640(2)
Cu	NA	1.984(2)	CA	NA	1.140(3)
Cu	NB	1.994(2)	CB	NB	1.163(3)
S1	C1	1.715(3)	S1′	C1′	1.719(3)
S1	C3	1.722(2)	S1′	C3′	1.721(2)
S2	C2	1.715(3)	S2′	C2′	1.725(3)
S2	C3	1.716(3)	S2′	C3′	1.717(3)
C1	C2	1.329(4)	C1′	C2′	1.325(4)
C1	H1	0.978(3)	C1′	H1′	0.897(3)
C2	H2	0.998(3)	C2′	H2′	0.924(3)
C3	C3′	1.388(3)			

The TTF molecules do not form columnar stacks, but are arranged in layers of slightly displaced stacked pairs which are 3.34 Å apart. A projection of a pair in the plane of the tetrathiafulvalene molecule (Fig. 2) illustrates the magnitude of the displacement. The perpendicular distance between pairs of TTF^{+} cations is 3.12 Å. The TTF^{+} cations in adjacent layers are oriented perpendicular to each other and are displaced by ½ along the *c* direction.

The electrical conductivity was of the order of 10^{-8} S cm^{-1} at room temperature for all crystal directions investigated. Clearly, the poor charge transport property is due to the absence of a TTF stack.

In the IR spectrum, the CN stretch of SCN showed a single strong band at 2090 cm^{-1}, although two crystallographically different thiocyanates are involved. Well defined vibrational bands attributable

TABLE 3. Bond Angles (°) for $(TTF)Cu(SCN)_2$

Atom	Atom	Atom	Angle (°)	Atom	Atom	Atom	Angle (°)
SA	Cu	SB	107.08(2)	Cu	SA	CA	102.40(9)
SA	Cu	NA	112.25(7)	Cu	SB	CB	97.10(8)
SA	Cu	NB	110.63(7)	SA	CA	NA	178.5(2)
SB	Cu	NA	112.79(7)	SB	CB	NB	179.4(2)
SB	Cu	NB	105.64(6)	Cu	NA	CA	162.9(2)
NA	Cu	NB	108.27(9)	Cu	NB	CB	156.7(2)
C1	S1	C3	95.1(1)	C1′	S1′	C3′	94.8(1)
C2	S2	C3	95.4(1)	C2′	S2′	C3′	94.1(1)
S1	C1	C2	117.5(2)	S1′	C1′	C2′	116.8(2)
C2	C1	H1	124.9(3)	C2′	C1′	H1′	123.2(3)
S1	C1	H1	117.4(3)	S1′	C1′	H1′	119.6(2)
S2	C2	C1	117.0(2)	S2′	C2′	C1′	118.2(2)
S2	C2	H2	121.0(3)	S2′	C2′	H2′	122.3(2)
C1	C2	H2	122.0(3)	C1′	C2′	H2′	119.3(3)
S1	C3	S2	115.0(1)	S1′	C3′	S2′	116.0(1)
S1	C3	C3′	123.0(2)	S1′	C3′	C3	121.2(2)
S2	C3	C3′	122.0(2)	S2′	C3′	C3	122.7(2)

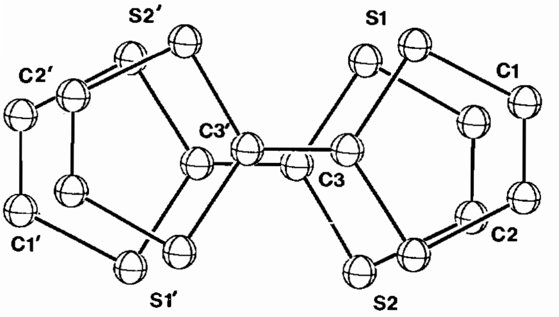

Fig. 2. ORTEP diagram with 50% probability ellipsoids showing displacement of pairs of tetrathiafulvalene molecules in (TTF)Cu(SCN)$_2$.

to TTF were observed at 3070(m), 3060(m), 3030(m), 1350(vs), 1260(m), 1098(w), 835(m), 826(m), 762(m), 756(m), 742(w), 725(m) and 716(s) cm^{-1}. Complete assignments have been performed for the vibrational band of TTF$^{+\cdot}$ radicals and TTF^0 neutral molecules [17]. In the IR spectra of TTF$^{+\cdot}$ compounds a vibronic interaction activates some A_g modes, which are otherwise IR inactive [17]: a broad strong band of the A_g-ν_3 mode appears at 1368 cm^{-1} in the IR spectrum of (TTF$^{+\cdot}$)Br. By reference to this result, the 1350 cm^{-1} band of (TTF)Cu(SCN)$_2$ can be assigned to the A_g mode (Fig. 3). The remaining main bands are attributable to the intrinsically IR active modes. The wavenumbers of the vibrational modes vary with the charge occupation of TTF. Especially, the B_{1u}-ν_{16} (CS stretch) and the B_{3u}-ν_{34} (CH bending) modes are sensitive to the charging effect: (TTF$^{+\cdot}$)Br exhibits ν_{16} at 836 cm^{-1} and ν_{34} at 705 cm^{-1}, whereas the ν_{16} and the ν_{34} modes of TTF neutral molecules appear at 781 and 639 cm^{-1}, respectively [17]. (The normal modes are numbered following ref. 17.) The 835 and 716 cm^{-1} bands of (TTF)Cu(SCN)$_2$ are close to the wavenumbers of the ν_{16} and ν_{34} modes of TTF$^{+\cdot}$, respectively. This shows that the TTF of (TTF)Cu(SCN)$_2$ carries unit charge as presumed from the compound formula.

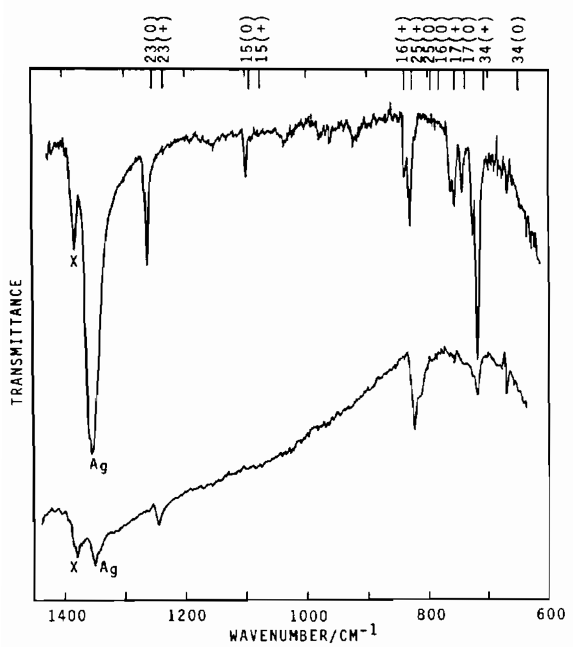

Fig. 3. Infrared spectra of Nujol mulls of (TTF)Cu(SCN)$_2$ (upper) and of (TTF)(SCN)$_{0.66}$ (lower). The Nujol bands are marked by X. The wavenumbers of the normal modes of (TTF$^{+\cdot}$)Br and TTF^0 are given at the top for comparison. The + and 0 after the mode number indicate the modes attributable to TTF$^{+\cdot}$ and TTF^0, respectively.

The copper 2p-core electron peak of the X-ray photoelectron spectrum of (TTF)Cu(SCN)$_2$ is shown in Fig. 4. On the basis of the measured Auger parameter, the copper peaks at 952.2 ± 0.2 eV and 932.4 ± 0.2 eV were assigned to the photoionization of the $2p_{1/2}$ and $2p_{3/2}$ electrons, respectively, of copper. Shake-up satellites due to copper(II) are not present, therefore, (TTF)Cu(SCN)$_2$ is not a mixed valence complex as are several TTF copper halides [1]. The copper is present exclusively as copper(I). Figure 5 shows the peak due to the unresolved sulfur $2p_{1/2}$ and $2p_{3/2}$ peaks with a maximum intensity at 164.8 ± 0.2 eV. A shoulder is clearly visible on the low binding energy side of the peak, suggesting the presence of at least two types of sulfurs. The binding energy of the maximum agrees with that found for other TTF copper halides [1]. The larger peak can be assigned to the four TTF$^{+\cdot}$ sulfurs, while the shoulder can be attributed to the two SCN$^-$ sulfurs. This assignment is consistent with the charging effect of the constituents on the binding energy. The width of the S 2p peak of mixed valence tetrathiafulvalene bromide and iodide has been shown by Ikemoto *et al.* [18] to be broader than that of a S 2p peak from either TTF^0 or TTF$^{+\cdot}$, because the peak is actually a superposition of the two oxidation states.

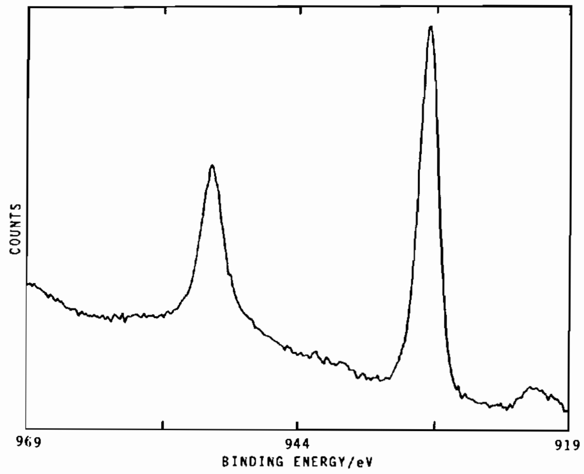

Fig. 4. X-ray photoelectron spectrum of Cu 2p peaks for (TTF)Cu(SCN)$_2$.

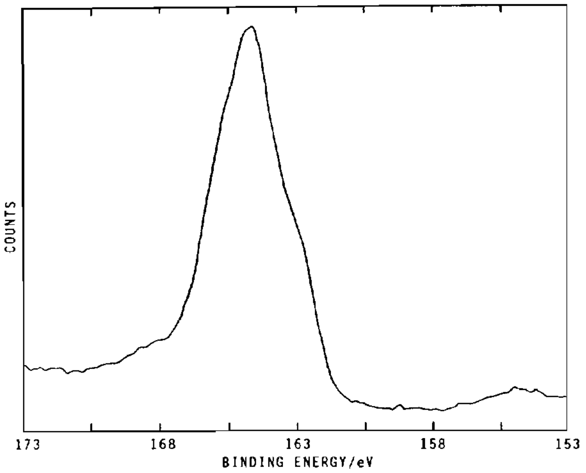

Fig. 5. X-ray photoelectron spectrum of S $2p_{1/2}$ and $2p_{3/2}$ peaks for $(TTF)Cu(SCN)_2$.

The FWHM of the TTF copper thiocyanate complex is 3.2 eV, which is at the upper limit for the FWHM of mixed oxidation state complexes. However, the presence of the thiocyanate sulfur 2p peak contributes significantly to the half width.

The compound exhibited no ESR signal, although it should contain paramagnetic species. The interplanar distance between paired TTF^{+} ions is small so that the unpaired electrons are strongly coupled to form a singlet state.

Black Needles, $(TTF)(SCN)_{0.66}$

A complete structural study was unsuccessful for $(TTF)(SCN)_{0.66}$, because the inorganic ions are disordered. Figure 6 shows the ORTEP packing diagram for the tetrathifulvalene molecules in the unit cell. Table 4 contains the final positional and isotropic thermal parameters. Table 5 contains the bond lengths and bond angles. The presence of incommensurate lattices of inorganic ions has been reported for some conducting TTF complexes such as $(TTF)Br_{0.71-0.76}$ [19], $(TTF)_7I_5$ [20], $(TTF)(SCN)_{0.55}$ [15], and $(TTF)_2CuCl_2$ [6]. Extensive studies performed on the bromide and the iodide have concluded that the TTF molecules and the halide ions individually construct monoclinic superlattices [19, 20]. The projection along the TTF stack, however, has a tetragonal symmetry.

TABLE 4. Positional Parameters[a] and Isotropic Thermal Parameters[b] for $(TTF)(SCN)_{0.66}$

Atom	x	y	z	B (Å^2)
SA	0.000	0.000	0.000	53(3)
S1	0.30599(6)	−0.00967(6)	0.7493(5)	4.51(1)
C1	0.2604(2)	−0.1568(3)	0.742(3)	5.31(7)
C2	0.4564(2)	−0.0424	0.750	3.52(5)
H1	0.333	0.332	0.240	5.000

[a] Hydrogen atom was not refined. [b] Anisotropically refined atoms are given in the form of the isotropic equivalent thermal parameter defined as: $8\pi^2(U_{11} + U_{22} + U_{33})/3$.

TABLE 5. Bond Lengths (Å) and Angles (°) for $(TTF)(SCN)_{0.66}$

Atom	Atom	Distance (Å)	Atom	Atom	Atom	Angle
S1	C1	1.729(3)	C1	S1	C2	94.92(9)
S1	C2	1.728(2)	S1	C1	C1	117.7(1)
C1	C1	1.316(5)	S1	C2	S1	114.9(1)
C2	C2	1.366(3)	S1	C2	C2	122.71(3)
C1	H1	1.054(2)				

Three isomorphic structures have been reported for materials with the formula $TTF(SCN)_{0.55-0.58}$ [15, 21, 22] and one for $(TTF)Cu_xCl_y$ [23]. Wudl *et al.* [15] have explained the molecular arrangements of $(TTF)(SCN)_{0.55}$ by reference to $(TTF)_7I_5$. The TTF molecules lie parallel to the *xy* plane and stack along the *z* direction in a face-to-face manner. The interplanar distance between TTF molecules is the length of the *c* axis of the tetragonal lattice. The TTF molecules in adjacent stacks are rotated 90° with respect to each other, and are displaced ½ along the

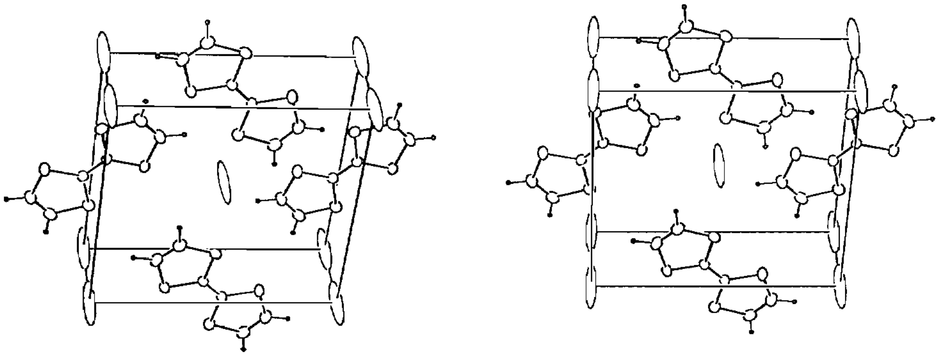

Fig. 6. ORTEP diagram for the tetrathiafulvalene molecules in the unit cell of $(TTF)(SCN)_{0.66}$.

TABLE 6. Comparison of Lattice Parameters for (TTF)-$(SCN)_x$

Formula	*a*	*c*	Reference
$(TTF)(SCN)_{0.66}$	11.225(1)	3.631(1)	this work
$(TTF)(SCN)_{0.58}$	11.11	3.61(1)	21
$(TTF)(SCN)_{0.57}$	11.154(3)	3.607(2)	22
$(TTF)(SCN)_{0.55}$	11.205(5)	3.632(2)	15
$(TTF)Cu_xCl_y$	11.17(5)	3.646(2)	23

c axis. Since the cell parameters of $(TTF)(SCN)_{0.66}$ are almost identical with the corresponding values of $(TTF)(SCN)_x$ (Table 6), the former can be assumed to be isostructural with the latter. The electron density in $(TTF)(SCN)_{0.55}$ is not uniform along the *c* axis and can be approximated by randomly oriented thiocyanate anions. The compound represented as $(TTF)(SCN)_{0.58}$ [21] showed two distinct spacings along the *c* axis, one corresponding to the TTF spacing and one to the SCN^- spacing. Somoano *et al.* [21] assert that the stoichiometry of the material they studied was significantly different from the material Wudl *et al.* used. $(TTF)(SCN)_{0.57}$ [22] showed uniform cylindrical symmetry along the *c* axis as did $(TTF)(SCN)_{0.66}$. The variation in the stoichiometries among these compounds probably results from subtle differences in the conditions under which they were crystallized.

The ESR spectrum was recorded on a single crystal that was mounted on a uniaxial goniometer so that the needle axis was perpendicular to the goniometer axis. When the needle axis (*i.e.* the crystal *c* axis) was parallel to the external field H_0, an asymmetric signal was observed with $g = 2.004$ and W_{pp} (peak-to-peak width) = 8 G. When the *c* axis was perpendicular to H_0, the values of g and W_{pp} were 2.007 and 12 G, respectively. The peak height of the low-field-side lobe of the observed derivative curve was twice as large as that of the high-field-side lobe, and the peak height ratio was angle-independent. The smallest g value was observed for c parallel to H_0. In π radical systems, the molecular g tensor has the smallest component along the axis that is perpendicular to the molecular plane [24]. Accordingly, the ESR result suggests that the TTF molecules stack along the *c* axis. This is consistent with X-ray crystallographic data.

The IR spectrum exhibited an intense broad band extending from 4000 to *ca.* 900 cm^{-1}, and vibrational bands are masked by this intense band. A similar spectrum has been observed for electroconductive TTF complexes and also for tetracyanoquinodimethane complexes [1, 25, 26]. The intense band has been interpreted on the basis of an electronic absorption [27]. The CN stretch of SCN was observed as a very weak band at 2090 cm^{-1}. Below the band edge of the absorption band, a well defined vibrational band appeared at 822 cm^{-1} with a shoulder (Fig. 3). For the $(TTF)_nCuX_2$ complexes that involve a strong intermolecular interaction between TTF moieties, a linear relation has been established between the wavenumber of the ν_{16} mode and the charge occupation of TTF [1]:

$$\nu_{16} = 792 + 51\rho \ (cm^{-1})$$

where ρ is the mean charge that resides on each TTF. The calculated value of ν_{16} for $(TTF)(SCN)_{0.66}$ using this equation gives a value of 826 cm^{-1}, which agrees well with the wavenumber of the observed band. This suggests that the TTF moiety carries a fractional charge as expected from the compound formula.

The electrical conductivity along the needle axis was 100–700 S cm^{-1} at 300 K, depending on the sample crystals. The conductivity may be extremely sensitive to crystal imperfection. The typical temperature dependence is shown in Fig. 7. A metallic behavior was observed above *ca.* 200 K, and below this temperature a metal-insulator transition occurred. This temperature dependence closely resembles that of $(TTF)(SCN)_{0.55}$ [15]. Temperature cycling during conductivity measurements resulted in the degradation of the electrical properties: a crystal once cooled showed a lower room temperature conductivity than that before cooling, and the

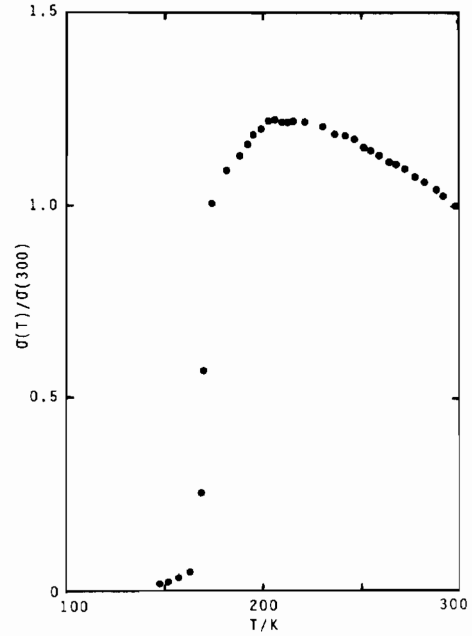

Fig. 7. The typical temperature dependence of the electrical conductivity $\sigma(T)/\sigma(300)$ of $(TTF)(SCN)_{0.66}$ along the TTF stack direction. The absolute conductivity $\sigma(300)$ at 300 K was in the range 100–700 S cm^{-1} depending on sample crystals.

temperature of the maximum conductivity became higher. Thus, the crystal was highly susceptible to thermal shock.

Discussion

The electrochemical oxidation of TTF yielded two kind of compounds: (TTF)Cu(SCN)$_2$ and (TTF)(SCN)$_{0.66}$. In order to increase the solubility of CuSCN in tetrahydrofuran, it was necessary to use a 2:1 NH$_4$SCN/CuSCN solution. In solution, [Cu(SCN)$_3$]$^{2-}$ that may be formed by mixing NH$_4$SCN and CuSCN in the mole ratio 2:1 is partially dissociated to [Cu(SCN)$_2$]$^-$ and SCN$^-$; no TTF complex is formed with the trithiocyanatocuprate.

The electrical and spectroscopic properties of the two compounds are quite different. This is related to the difference in the molecular arrangements of TTF. One of the requirements for the formation of highly conducting charge-transfer complexes is the close-packed stack of planar molecules that have a fractional charge [28]. This important requirement is not realized in (TTF)Cu(SCN)$_2$ which is a poor conductor. In the crystal, the pairs of $\mathrm{TTF}^{\dot{+}}$ are segregated by copper–thiocyanate sheets, and unit charge resides on each TTF.

The mean charge density on TTF in (TTF)(SCN)$_{0.66}$ is *ca.* 20% larger than of (TTF)(SCN)$_{0.55}$. This difference, however, does not influence the interplanar TTF distance (*i.e.* the length of the *c* axis) and the charge transport property. In the (TTF)(SCN)$_{0.55}$ crystal, only about 40% of the volume of the SCN channel is filled by the inorganic ions [15]. The channel has a 'free volume' that potentially accommodates more SCN$^-$ ions. About 20% more SCN$^-$ ions are accommodated in (TTF)(SCN)$_{0.66}$, but this results in a very small increase (*ca.* 0.3%) of the unit cell volume. This, however, does not imply that the channel can be filled up with SCN$^-$ ions. The free volume is required for the stabilization of the fractional charge occupation in nonstoichiometric compounds.

Supplementary Material

Listings of the structure factors are available from author Q.F.

Acknowledgement

The work at the Universidad de Sonora was supported by the Dirección General de Investigación Científica y Superación Académica, SEP, Mexico (Grant No. C87-08-0151-2).

References

1 M. B. Inoue, M. Inoue, Q. Fernando and K. W. Nebesny, *Inorg. Chem., 25* (1986) 3976.
2 M. B. Inoue, C. Cruz-Vazquez, M. Inoue, Q. Fernando and K. W. Nebesny, *Inorg. Chem., 26* (1987) 1462.
3 A. R. Siedle, G. A. Candela, T. F. Finnegan, R. P. Van Duyne, J. T. Cape, G. F. Kokoszka, P. M. Woyciejes and J. A. Hashmall, *Inorg. Chem., 20* (1981) 2635.
4 M. Honda, C. Katayama, J. Tanaka and M. Tanaka, *Acta Crystallogr., Sect. C, 41* (1985) 197.
5 M. Honda, C. Katayama, J. Tanaka and M. Tanaka, *Acta Crystallogr., Sect. C, 41* (1985) 688.
6 M. Inoue, M. B. Inoue, C. Cruz-Vazquez, S. Roberts and Q. Fernando, *Synth. Met., 19* (1987) 641.
7 M. Tanaka, A. Kawamoto, J. Tanaka, M. Sano, T. Enoki and H. Inokuchi, *Bull. Chem. Soc. Jpn., 60* (1987) 2531.
8 M. B. Inoue, C. Cruz-Vazquez, M. Inoue, G. J. Pyrka, K. W. Nebesny and Q. Fernando, *Synth. Met., 22* (1988) 231.
9 U. Geiser, H. H. Wang, C. E. Hammond, M. A. Firestone, M. A. Beno, K. Carlson, L. Nuñez and J. A. Williams, *Acta Crystallogr., Sect. C, 43* (1987) 656.
10 M. Inoue, M. B. Inoue, T. Asaji and D. Nakamura, *Solid State Commun., 63* (1987) 807.
11 M. Inoue and D. Nakamura, *Synth. Met., 20* (1987) 229.
12 R. Colton and J. H. Canterford, *Halides of the First Row Transition Metals*, Wiley, London, 1969.
13 D. T. Cromer and J. T. Waber, *International Tables for X-ray Crystallography*, Vol. IV, Kynoch Press, Birmingham, 1974, Table 2.2B.
14 D. T. Cromer, *International Tables for X-ray Crystallography*, Vol. IV, Kynoch Press, Birmingham, 1974, Table 2.3.1.
15 F. Wudl, D. E. Schafer, W. M. Walsh, Jr., L. W. Rupp, F. J. DiSalvo, J. Waszczak, M. L. Kaplan and B. A. Thomas, *J. Chem. Phys., 66* (1977) 377.
16 M. DiVaira and F. Mani, *J. Chem. Soc., Dalton Trans.*, (1985) 2327.
17 R. Bozio, I. Zanon, A. Giralando and C. Pecile, *J. Chem. Phys., 71* (1979) 2282.
18 I. Ikemoto, M. Yamada, T. Sugano and H. Kuroda, *Bull. Chem. Soc. Jpn., 53* (1980) 1871.
19 S. J. LaPlaca, P. W. R. Carfield, R. Thomas and B. A. Scott, *Solid State Commun., 17* (1975) 635.
20 J. J. Daly and F. Sanz, *Acta Crystallogr., Sect. B, 31* (1975) 620.
21 R. B. Somoano, A. Gupta, V. Hadek, M. Novotny, M. Jones, T. Datta, R. Deck and A. M. Hermann, *Phys. Rev. B, 15* (1977) 595.
22 H. Kobayashi and K. Kobayashi, *Bull. Chem. Soc. Jpn., 50* (1977) 3127.
23 F. Sanz, *An. Fiz.*, (1976) 43.
24 A. Carrington and A. D. McLachlan, *Introduction to Magnetic Resonance*, Harper and Row, New York, 1967.
25 R. C. Wheland and J. L. Gillson, *J. Am. Chem. Soc., 98* (1976) 3916.
26 M. Inoue and M. B. Inoue, *J. Chem. Soc. Faraday Trans. 2, 81* (1985) 539.
27 M. J. Rice, L. Pietronero and P. Brüesch, *Solid State Commun., 21* (1977) 757.
28 A. J. Heeger and A. F. Garito, in H. J. Keller (ed.), *Low-Dimensional Cooperative Phenomena*, Plenum, New York, 1975, p. 89.